

# Afucosylated immunoglobulin G responses are a hallmark of enveloped virus infections and show an exacerbated phenotype in COVID-19

Short title: Afucosylated IgG responses

**Authors:** Mads Delbo Larsen<sup>1\*</sup>, Erik L. de Graaf<sup>1\*</sup>, Myrthe E. Sonneveld<sup>1\*</sup>, H. Rosina Plomp<sup>2</sup>, Federica Linty<sup>1</sup>, Remco Visser<sup>1</sup>, Maximilian Brinkhaus<sup>1</sup>, Tonći Šuštić<sup>1</sup>, Steven W. de Taeye<sup>1</sup>, Arthur E.H. Bentlage<sup>1</sup>, Jan Nouta<sup>2</sup>, Suvi Natunen<sup>3</sup>, Carolien A. M. Koeleman<sup>2</sup>, Susanna Sainio<sup>3</sup>, Neeltje A. Kootstra<sup>4</sup>, Philip J.M. Brouwer<sup>5</sup>, Rogier W. Sanders<sup>5</sup>, Marit J. van Gils<sup>5</sup>, Sanne de Bruin<sup>6</sup>, Alexander P.J. Vlaar<sup>6,7</sup>, Amsterdam UMC COVID-19 biobank study group, Hans L. Zaaijer<sup>7</sup>, Manfred Wuhrer<sup>2</sup>, C. Ellen van der Schoot<sup>1</sup>, Gestur Vidarsson<sup>1</sup>

## Affiliations:

<sup>1</sup> Department of Experimental Immunohematology, Sanquin Research, Amsterdam, The Netherlands, and Landsteiner Laboratory, Amsterdam UMC, University of Amsterdam, Amsterdam, The Netherlands;

<sup>2</sup> Center for Proteomics and Metabolomics, Leiden University Medical Center, Leiden, The Netherlands;

<sup>3</sup> Finnish Red Cross Blood Service, Helsinki, Finland;

<sup>4</sup> Department of Experimental Immunology, Amsterdam UMC, University of Amsterdam Amsterdam, The Netherlands;

<sup>5</sup> Department of Medical Microbiology, Amsterdam University Medical Centers (Location AMC), University of Amsterdam, Amsterdam, The Netherlands;

<sup>6</sup> Department of Intensive Care Medicine, Amsterdam UMC (Location AMC), University of Amsterdam, Amsterdam, The Netherlands;

<sup>7</sup> Department of Blood-borne Infections, Sanquin, Amsterdam, The Netherlands.

\*Contributed equally

26

27 **Abstract:**

28 IgG antibodies are crucial for protection against invading pathogens. A highly conserved N-  
29 linked glycan within the IgG-Fc-tail, essential for IgG function, shows variable composition in  
30 humans. Afucosylated IgG variants are already used in anti-cancer therapeutic antibodies for  
31 their elevated binding and killing activity through Fc receptors (FcγRIIIa). Here, we report that  
32 afucosylated IgG which are of minor abundance in humans (~6% of total IgG) are specifically  
33 formed against surface epitopes of enveloped viruses after natural infections or  
34 immunization with attenuated viruses, while protein subunit immunization does not elicit  
35 this low fucose response. This can give beneficial strong responses, but can also go awry,  
36 resulting in a cytokine-storm and immune-mediated pathologies. In the case of COVID-19,  
37 the critically ill show aggravated afucosylated-IgG responses against the viral spike protein. In  
38 contrast, those clearing the infection unaided show higher fucosylation levels of the anti-  
39 spike protein IgG. Our findings indicate antibody glycosylation as a potential factor in  
40 inflammation and protection in enveloped virus infections including COVID-19.

41 **Main Text:**

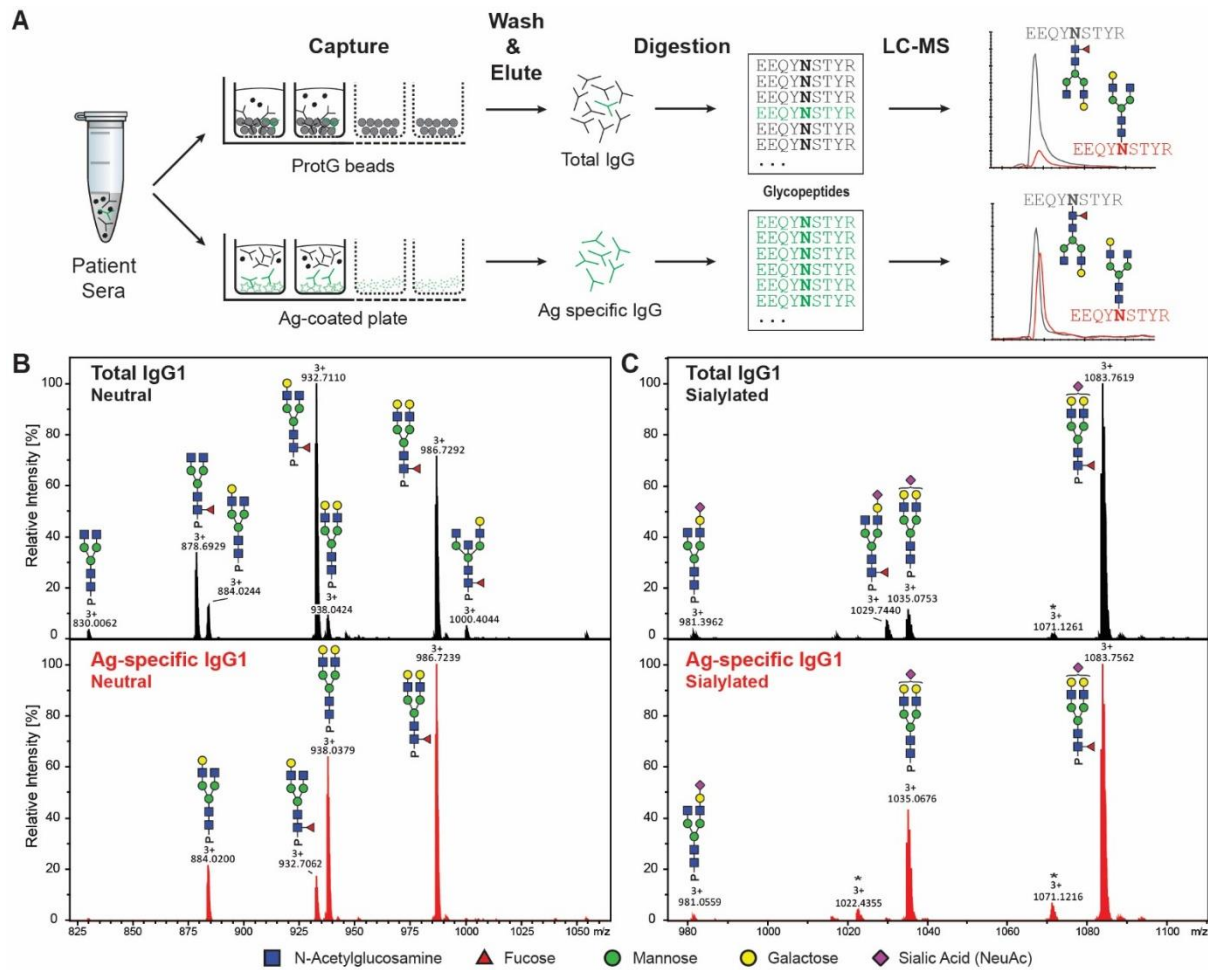
42 Antibodies have long been considered functionally static, mostly determined by their isotype  
43 and subclass. The presence of a conserved N-linked glycan at position 297, in the so called  
44 constant Fc-domain of IgG, is essential for effector functions (1–3). Moreover, it is now  
45 generally accepted that the composition of this glycan is highly variable and has functional  
46 consequences (2–4). This is especially true for the core fucose attached to the Fc glycan. The  
47 discovery that IgG variants without core fucosylation cause elevated antibody dependent  
48 cellular cytotoxicity (ADCC), via increased IgG-Fc-receptor IIIa (FcγRIIIa) affinity (5, 6),  
49 resulted in next-generation glyco-engineered monoclonal antibodies (mAb) without core  
50 fucosylation for targeting tumors (7).

51 Generally, changes in the Fc glycans are associated with age, sex and autoimmune diseases  
52 (8). Serum IgG are highly fucosylated at birth and slightly decrease to ~94% fucosylation at  
53 adulthood (9). Until now, no strong clues on how IgG core fucosylation is controlled have  
54 come forward.

55 We have previously observed that alloantibodies against red blood cells (RBC) and platelets  
56 show remarkably low IgG-Fc-fucosylation in most patients, even down to 10% in several  
57 cases (10–12), whereas the overall serum IgG Fc-fucosylation show consistently normal high  
58 levels. Moreover, we have reported the lowered IgG-Fc fucosylation to be one of the factors  
59 determining disease severity in pregnancy associated alloimmunizations, resulting in  
60 excessive thrombocytopenia's and blood cell destruction when targeted by afucosylated  
61 antibodies (11–13). In addition to the specific afucosylated-IgG response against platelets  
62 and RBC antigens, this response has also been identified against HIV and Dengue virus (14,  
63 15), but not for any other immune response so far, e.g. not against inactivated influenza,  
64 pneumococcal, meningococcal or tetanus vaccines (16, 17). Interestingly, low core  
65 fucosylation of anti-HIV antibodies has been suggested to be a feature of elite controllers of  
66 infection, and for Dengue it has been associated with enhanced pathology due to excessive  
67 FcγRIIIa-activation (14, 15).

68 Inspired by the similarities between the unique afucosylated IgG responses in various  
69 alloimmune responses (10–12, 18), HIV (15) and Dengue(14) – all being directed against  
70 surface exposed and membrane embedded proteins -we analyzed IgG glycosylation in anti-  
71 human platelet and red-blood cell alloimmune responses as well as in natural infections by  
72 other enveloped viruses, including HIV, cytomegalovirus (CMV), and SARS-CoV-2. Similarly,  
73 we also assessed for a non-enveloped virus (Parvovirus B19), vaccination with a protein  
74 subunit, and live attenuated enveloped viruses, to test if the antigen context is indeed an  
75 important determinant for IgG-Fc glycosylation.

76 To investigate the Fc-glycosylation of total- and antigen-specific antibodies, first IgG from  
77 >400 human serum samples was affinity-purified using protein G affinity beads and  
78 immobilized antigens, respectively. Thereafter, isolated IgG was digested with trypsin and  
79 resulting IgG1-Fc-glycopeptides were analyzed with liquid chromatography-mass  
80 spectrometry (LC-MS) (Fig. 2A) (11, 16, 18). Subsequently, intensities were extracted and IgG-  
81 glycosylation profiles were calculated (Fig. 1B-C).



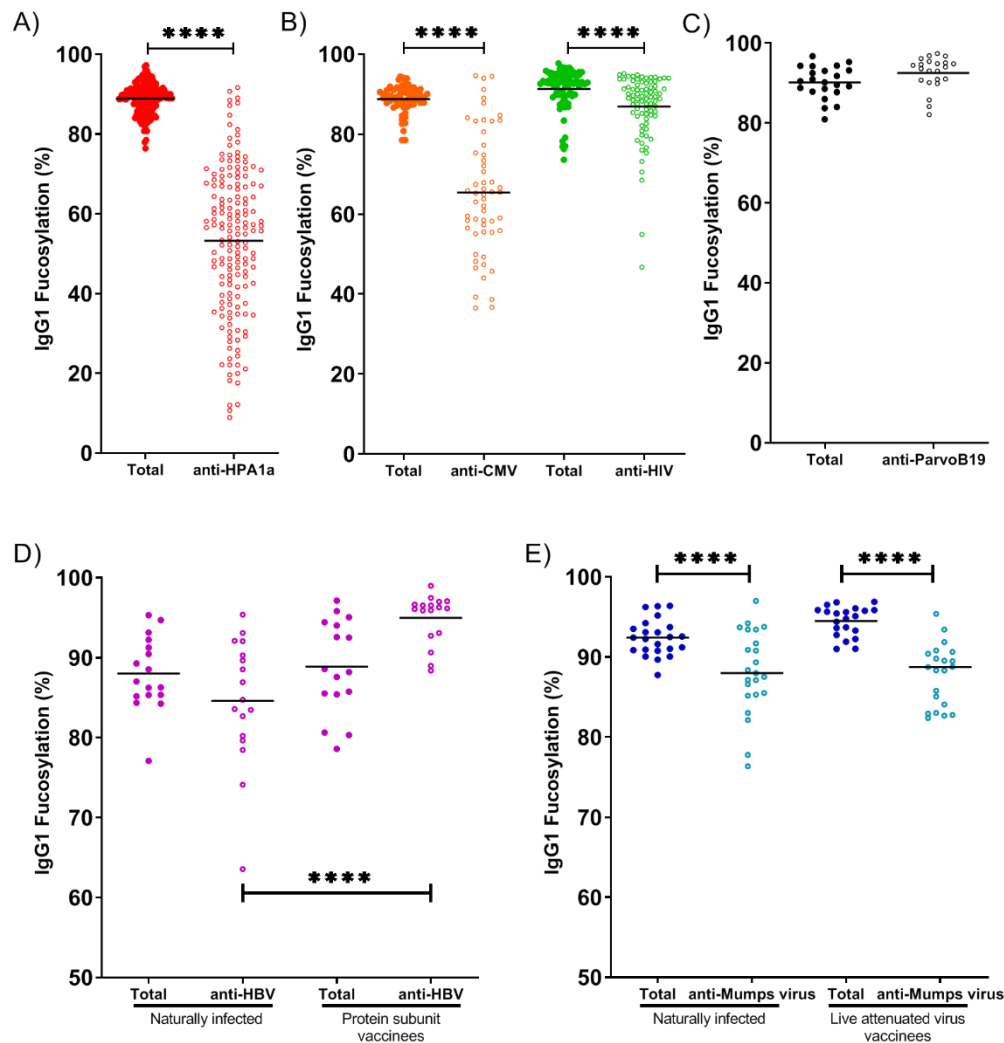
82

83 **Fig. 1. Flowchart of antibody specific IgG1 glycosylation analysis and mass spectrometric**  
 84 **analysis. A)** Antibodies from sera were captured using ProteinG beads and antigen-coated  
 85 96-well plates resulting in total and antigen-specific IgG fractions, respectively. Thereafter,  
 86 isolated IgGs were digested with trypsin and the resulting glycopeptides were analyzed by  
 87 nano liquid chromatography-coupled mass spectrometry. **B,C)** Representative mass spectra  
 88 of glycopeptides encompassing the Fc glycosylation site Asn297. Neutral (**B**) and sialylated  
 89 (**C**) IgG1 glycopeptides are shown from a single patients' total (upper panel, in black) and an-  
 90 tigen-specific (lower panel, in red) IgG1 fraction. Asterisks indicate non-Fc glycopeptides.

91

92 Antigen-specific antibodies against the alloantigen human platelet antigen (HPA)-1a showed  
 93 a strong decrease in fucosylation (Fig. 2A), similar to our previous findings for other  
 94 alloantigens (11, 18).

95



96

97 **Fig. 2 Foreign membrane protein antigens, such as envelope proteins of (attenuated) en-**  
 98 **veloped viruses or alloantigens can trigger afucosylated IgG responses.** IgG1-Fc Fucosyla-  
 99 tion levels of total (filled circles) and antigen-specific (open circles) antibodies are shown for  
 100 each differently color-coded group of antigens: **A)** alloantigen HPA-1a; **B)** viral envelope anti-  
 101 gens from CMV and HIV; **C)** non-enveloped viral antigens from Parvo B19. **D)** IgG Fc-fucosyla-  
 102 tion levels of total and antigen-specific IgGs in individuals naturally infected with Hepatitis B  
 103 Virus (left) or vaccinated with recombinant soluble HBsAg (right). **E)** Fc-fucosylation levels of  
 104 total and ag-specific IgGs in individuals naturally infected with mumps virus (left), or vac-  
 105 cinated with live attenuated mumps virus (left) . Statistical analysis was performed as paired  
 106 t-test for A,B, and C and as a one-way ANOVA Sidak's multiple comparisons test comparing  
 107 total IgG to antigen-specific IgG within groups, and same specificity IgG between groups, for  
 108 D and E. Only statistically significant differences are shown. \* =  $p < 0.1$ , \*\* =  $p < 0.01$ , \*\*\* =  
 109  $p < 0.001$ , \*\*\*\* =  $p < 0.0001$ .

110 Analogous to the platelet and Red Blood cell alloantigens (10–12, 18), the response to these  
 111 enveloped viruses also showed significant afucosylation of the antigen-specific IgG (Fig.2B),  
 112 while the afucosylation was absent against the non-enveloped virus Parvo B19 (Fig.2C). Of

113 note, total IgG showed high fucosylation levels throughout (Fig.2A-C), underlining that the  
114 majority of human IgG responses consists of fucosylated IgG responses (11, 16, 19). The  
115 extent of the response to the enveloped viruses was highly variable, both between  
116 individuals and between the types of antigen, which is in agreement with the variable  
117 tendency of different RBC-alloantigens to induce an afucosylated response (18).  
118 Afucosylation was particularly strong for CMV and to a lesser degree for HIV (Fig. 2B). The  
119 anti-HIV response is in line with what was previously described by Ackerman et al., showing a  
120 decreased fucosylation of HIV-specific IgG compared to total IgG (15). Other glycan traits are  
121 depicted in Fig. S1.

122 To test whether some individuals had a greater intrinsic capacity to generate an afucosylated  
123 IgG response than others, we compared IgG-Fc fucosylation levels formed against different  
124 antigens within the same individual. No correlation in IgG1 Fc fucosylation was observed  
125 between anti-HPA1a and anti-CMV (Fig. S2), nor between anti-HIV and anti-CMV antibodies  
126 in the same individual (Fig. S2), suggesting that the level of afucosylation is not determined  
127 by a general host factor such as genetics but is rather stochastic or multifactorial, with the  
128 specific triggers remaining obscure.

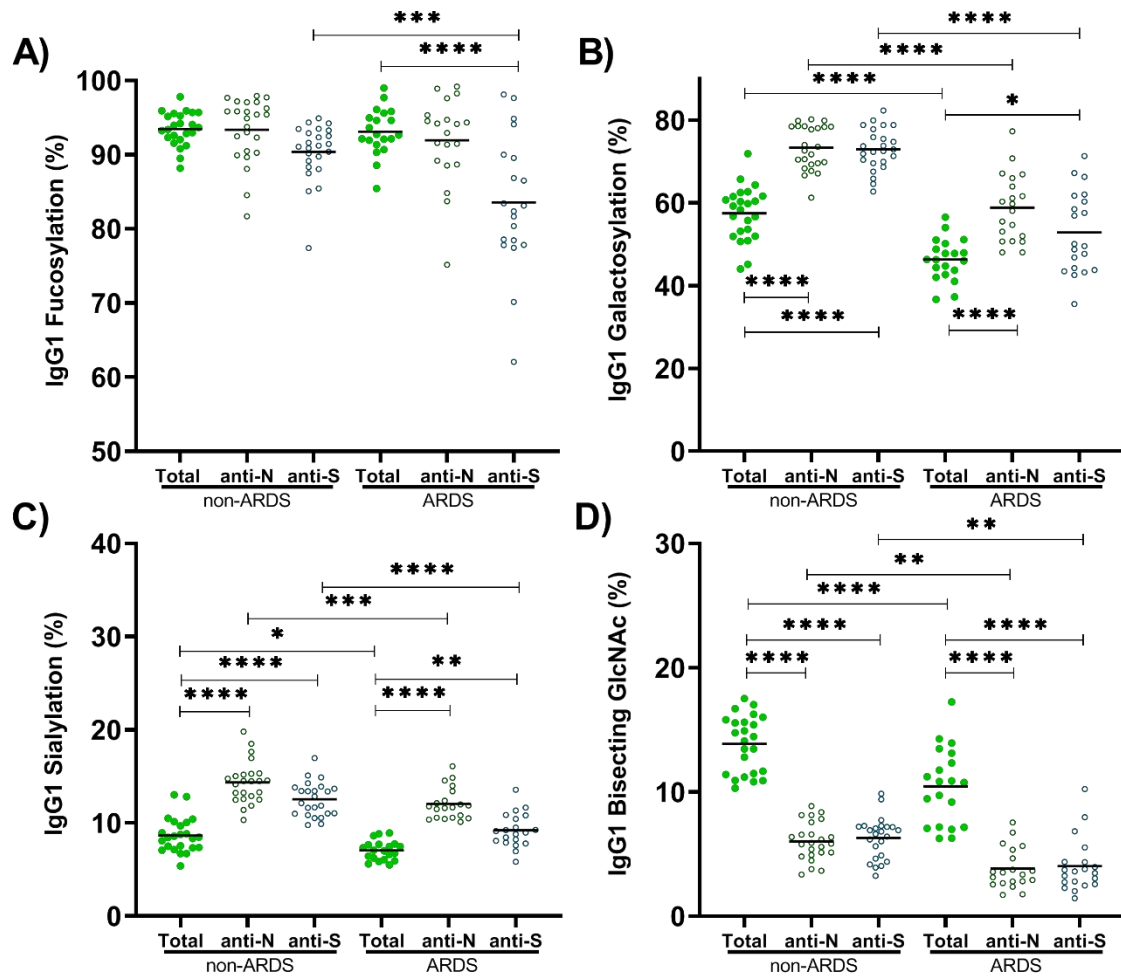
129

130 To further investigate the immunological context by which potent low fucosylated IgG is  
131 formed, we compared immune responses to identical viral antigens in different contexts.  
132 First, we compared Hepatitis B surface antigen (HBsAg)-specific antibody glycosylation in  
133 humans naturally infected with Hepatitis B Virus (HBV) or vaccinated with the recombinant  
134 HBsAg protein (Fig. 2D). Whereas total-IgG1 fucosylation levels were similar in the two  
135 groups, anti-HBsAg IgG1 fucosylation was elevated in individuals vaccinated with the HBsAg  
136 protein both compared to the fucosylation of total IgG of both groups and antigen-specific  
137 IgG of the naturally infected group. The finding that HBsAg-specific antibodies in individuals  
138 that cleared a natural infection showed lowered Fc-fucosylation compared to protein subunit  
139 vaccination strongly suggests that a specific context for the antigenic stimulus is required for  
140 afucosylated-IgG responses.

141 We then compared antiviral-IgG responses against Mumps- and Measle viruses-formed after  
142 a natural infection or vaccination with live attenuated viruses. Unlike the HBV protein subunit  
143 vaccine, both attenuated live vaccines showed a similar Ag-specific Fc-fucosylation compared  
144 to their natural infection counterpart (Fig. 2E, Fig. S3). Both showed reduction, with a more  
145 prominent difference for the mumps response (Fig. 2E, Fig S3). Other glycan traits for anti-  
146 measles and anti-mumps are shown in Fig. S1.

147 We then tested if this type of response also plays a role in patients with SARS-CoV-2 (COVID-  
148 19). Symptoms of COVID-19 are highly diverse, ranging from asymptomatic or mild self-  
149 limiting infection to a severe airway inflammation leading to respiratory distress, often with a  
150 fatal outcome(20, 21). Both extreme trajectories, follow similar initial responses: patients  
151 have approximately a week of relatively mild symptoms, followed by a second wave that  
152 either clears the disease or leads to a highly-aggravated life-threatening phenotype (20, 21).  
153 Both the timing of either response type and the differential clinical outcome suggests  
154 different paths taken by the immune system to combat the disease. So far no clear evidence  
155 has emerged that can make a distinction between these two hypothetical immunological  
156 paths. In accordance with our theory and responses seen in other enveloped viruses, anti-S  
157 IgG responses against SARS-CoV-2 spike protein (S), expressed on cell surface/viral envelope,  
158 were strongly skewed towards low core fucosylation, while those against the nucleocapsid  
159 protein (N), not expressed on cell surface/viral envelope, was characterized with high level  
160 of fucose. Importantly, the afucosylated anti-S IgG-responses of patients with Acute  
161 Respiratory Distress Syndrome (ARDS) hospitalized in intensive care units were significantly  
162 lower than in convalescent plasma donors consisting of individuals who were asymptomatic  
163 or had relative mild symptoms (non-ARDS) (Fig. 3A).





164

165 **Figure 3: Fucosylation levels of anti-S IgG1, but not anti-N, are significantly decreased in**  
 166 **critically ill COVID-19 patients . A)** Fucosylation was significantly lowered for ARDS patients  
 167 for anti-S, but not in non-ARDS donors naturally clearing the infection. Anti-N responses were  
 168 similar to total IgG. **B)** Galactosylation, was increased for both anti-N and anti-S in non-ARDS  
 169 donors as well as ARDS patients **C)** Sialylation shows similar patterns as galactosylation, and  
 170 **D)** Bisection was very low for both anti-N and anti-S in both patient groups. Statistical  
 171 analysis was performed as a one-way ANOVA with Sidak's multiple comparisons test,  
 172 comparing total IgG to antigen-specific IgG within groups, and same specificity IgG between  
 173 groups. Only statistically significant differences are shown. \*= p<0.1, \*\*= p<0.01, \*\*\*=  
 174 p<0.001, \*\*\*\*= p<0.0001

175 This lowered fucosylation of the anti-S was not a general issue of the inflammation as total  
 176 IgG-fucosylation levels were similar in the two groups and to what has been reported in the

177 general population (~94%) (11, 16). In addition, IgG galactosylation of both anti-S and anti-N  
178 responses tended to be higher than seen in total IgG, compatible with increased  
179 galactosylation observed in active or recent immunization (16, 22). However, IgG  
180 galactosylation levels in general were lower in the ARDS patients, perhaps suggesting lower  
181 capacity to clear the infection by reduced complement activity (23). This may be a reflection  
182 of a slight age difference in these two groups (non-ARDS donors median 53±12,  
183 ARDS patients 61±7.9), as galactose generally decreases slightly with advancing age (9, 19).  
184 More importantly, the lowered fucosylation in the anti-S responses of the ARDS patients,  
185 strongly suggest a pathological role through FcγRIIIa, similar to what was previously  
186 proposed for Dengue (14). In Dengue, non-neutralizing antibodies formed to previous  
187 infections of other Dengue serotypes, also tend to have low level of core-fucosylated IgG  
188 and, as they are not capable of preventing infection, leading to aggravated Dengue-disease  
189 due to FcγRIIIa-mediated overreactions by immune cells (14).

190

191 In conclusion, our results show a pattern of afucosylated IgG1 immune responses against  
192 membrane-embedded antigens such as surface membrane proteins of allo-antigens on blood  
193 cells or on enveloped viruses, in contrast to soluble protein antigens and non-enveloped  
194 viruses for which immune responses with high levels of IgG1 fucosylation are consistently  
195 observed. We hypothesize that antigen-presenting membranes are directly sensed by B cells  
196 combining at least two signals provided by the B cell receptor and a yet unknown host  
197 receptor-ligand pair, not occurring for soluble proteins, internal protein of enveloped viruses  
198 or non-enveloped viruses(Fig. 4).

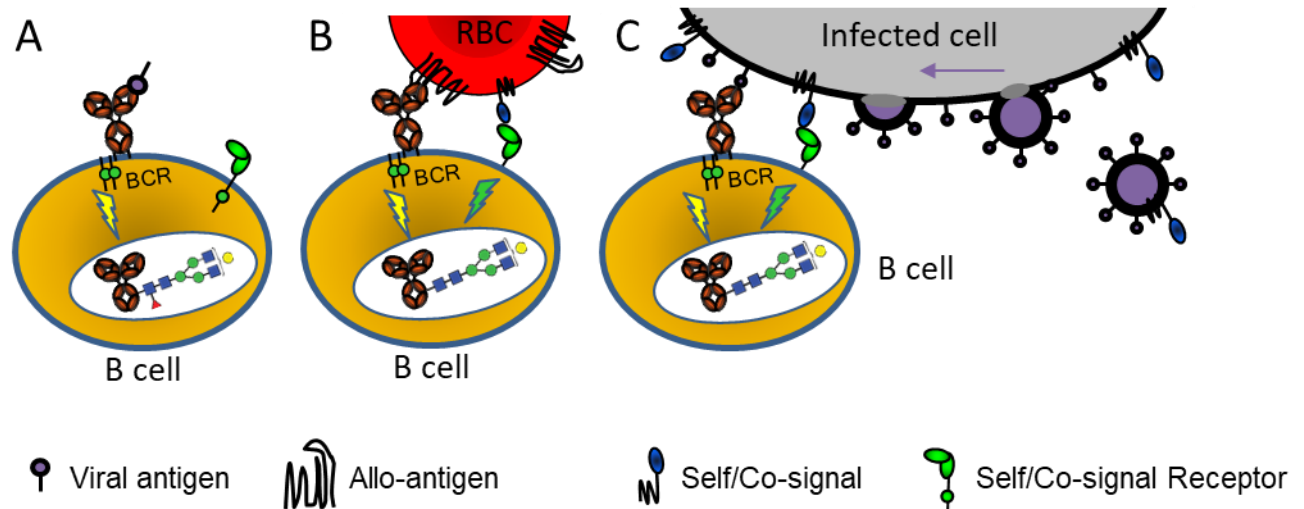


**Fig. 4 Hypothetical model explaining how the context of antigen can lead to altered im-**

**mune signaling, giving rise to altered IgG-glycosylation** **A)** Immune response to soluble protein antigen: B-cell receptor (BCR, a membrane immunoglobulin) is activated, resulting in the production of normal fucosylated antibodies. **B)** Immune response to allo-antigens: Paternal allo-antigen on a Red Blood Cell (RBC) recognized by the BCR, and possibly by a yet unknown immune regulatory receptor-ligand pair providing a signal for self. **C)** Immune response to enveloped viral infection: Recognition of enveloped-virus infected cells by B cells is similar as for cellular-alloantigen recognition. The initial recognition can potentially occur towards enveloped-virally infected cells and possibly after viral assembly (far right). The proposed signaling in b-c) causes altered glyco-programming of the B cells culminating in a unique IgG-response characterized by a low fucosylation (fucose red triangle) and enhanced ADCC. The model potentially explains both why immune response to soluble proteins, non-enveloped viruses and cellular pathogens such as bacteria is different to responses to enveloped-viruses and why immune responses to allo-antigens mimic that of an enveloped viral infection.

215 Alternatively, the differential recognition may be more complex and require additional

216 interactions from antigen-presenting cells, T cells and/or cytokines. Importantly, our studies

217 imply that a membrane context may be necessary but not always sufficient to trigger an

218 immune response with high levels of afucosylated IgG. (18). This translates into a vast spread

219 of afucosylation levels between individuals as well as for distinct responses of the same

220 individual against different antigens. The large difference in the level of antigen-specific

221 afucosylated responses observed between patients contributes to the variability of disease

222 severity, as has been shown for the neonatal alloimmune cytopenias (11, 12, 18), Dengue

223 (14) and now also for COVID-19. This underscores the significance for diagnosis of possible

224 disease trajectories and guides future treatments aimed at minimizing this FcγRIIIa-stimulus.

225 Importantly, when IgG afucosylation does occur, the final outcome, results in a potent  
226 immune response, honed for destruction of targets cells by FcγRIIIa-expressing NK cells,  
227 monocytes and macrophages but also FcγRIIIb-expressing granulocytes. This can be desired  
228 in some responses such as against HIV (15), which can be achieved with available attenuated  
229 enveloped viral vaccine shuttles (24) against difficult targets. On the other hand, this can also  
230 lead to an undesired exaggerated response, as is apparent for both Dengue (14) and COVID-  
231 19. This is exemplified in experiments in monkeys, where vaccination with Modified Vaccinia  
232 Ankara virus ferrying spike proteins of SARS-CoV lead to strong ADE response (25) mimicking  
233 pathologies in critically ill SARS-CoV2 patients (21). This suggests that a subunit protein  
234 vaccine to be a safer option as seen in rat models for SARS-CoV2 (26), unless the vaccine also  
235 induces a strong neutralizing effect.

236 For COVID-19, the data suggest that afucosylation of anti-S IgG may contribute to the  
237 exacerbation of the disease in an subset of patient ending up in Intensive care units with  
238 ARDS. Thus although they can be protective, they might potentially behave as double-edged  
239 swords, and may contribute to the observed cytokine storm (27). As such this has direct  
240 consequences for improving current therapies with IVIg, convalescent plasma and the route  
241 taken towards vaccine development. In addition, the suggested role of afucosylated  
242 antibodies in the pathogenesis of COVID-19 might open new opportunities for therapy of this  
243 disease. Future attempts of generating high-titer COVID-19 immunoglobulin treatments,  
244 should preferably use plasma enriched in fucosylated anti-COVID-19 antibodies. These may  
245 outcompete afucosylated anti-SARS-CoV2 IgG-responses developing in the patients to avoid  
246 symptom escalation and promote virus neutralization.

247

248 **Materials and Methods:**

249 **Patient samples**

250 Healthy blood donor samples from Sanquin, Amsterdam, The Netherlands, were used to  
251 analyze ParvoB19 (n=22), Measle virus (n=21 natural infection, n=24 Live Attenuated  
252 vaccine), Mump virus (n=21 natural infection, n=24 Live Attenuated vaccine) and HBV  
253 antibodies (n=17 natural infection, n=16 HBsAg vaccination). Anti-HPA-1a samples have been  
254 described elsewhere (13). HIV-samples (n=80) from the Amsterdam Cohort Studies on HIV  
255 infection and AIDS (ACS) were used to analyze HIV-specific antibody glycosylation. SARS-CoV2  
256 patient samples from ICU patient from the Amsterdam UMC COVID study group were  
257 included, as well as from Sanquin blood donors found positive. The ACS have been  
258 conducted in accordance with the ethical principles set out in the declaration of Helsinki and  
259 all participants provided written informed consent. The study was approved by the Academic  
260 Medical Center institutional Medical Ethics Committee of the University of Amsterdam.

261 Peripheral blood samples from patients with HPA-1a alloantibodies and CMV-specific  
262 antibodies (n=62) were collected by the Finnish Red Cross Blood service, Platelet  
263 Immunology Laboratory, Helsinki, Finland.

264

265 **Purification of CMV-specific antibodies from sera**

266 CMV-specific antibodies were purified using antigen-coated plates (Serion ELISA classic,  
267 Cytomegalovirus IgG, Würzburg, Germany). Sera (20  $\mu$ L) diluted in specimen diluent (80  $\mu$ L)  
268 from kit was incubated for 1 hour at 37 °C degrees. Positive and negative controls from the  
269 kit and CMV-negative patients samples were used as controls. The plates were washed seven  
270 times: three times with 300  $\mu$ L wash-buffer from the kit, followed by two washed with the  
271 same volume Phosphate buffered saline (PBS) and deionized water. The bound antibodies  
272 were then eluted using 100  $\mu$ L of 100 mmol/l formic acid. No IgG was found in eluates from  
273 blank wells and CMV-negative patients samples.

274 **Purification of Measle- and Mump-virus specific antibodies from sera**

275 Ag-specific antibodies were purified using antigen-coated plates (Serion ELISA classic,  
276 Measles IgG and Mumps IgG, Würzburg, Germany). Sera (20  $\mu$ L) diluted in specimen diluent  
277 (80  $\mu$ L) from kit was incubated for 1 hour at 37 °C degrees. Positive and negative controls  
278 from the kit were used as controls. The plates were washed seven times: three times with  
279 300  $\mu$ L wash-buffer from the kit, followed by two washed with the same volume Phosphate  
280 buffered saline (PBS) and 50mM ammonium bicarbonate. The bound antibodies were then  
281 eluted using 100  $\mu$ L of 100 mM formic acid. IgG was found in the eluates of positive controls  
282 and no IgG was found in eluates from blank wells and negative control samples.

283

284 **Purification of HBV-specific antibodies from sera**

285 To isolate HBsAg specific antibodies from patients after infection and vaccination, HBs  
286 antigen-coated plates (ETI-AB-AUK-3, Diasorin, Schiphol-Rijk, The Netherlands) were used.  
287 Sera were diluted five times in specimen diluent from kit (20  $\mu$ L serum with 80  $\mu$ L diluent)  
288 and incubated for 1 hour at room temperature with shaking 450 r.p.m. (Heidolph Titramax  
289 100, Schwabach, Germany). HBV-naive and HBV-resolved samples from Sanquin, Amsterdam,  
290 The Netherlands were used as controls. Washing and eluting specific antibodies was done as  
291 described above for CMV-specific antibodies.

292

293 **Purification of HIV-specific antibodies from sera**

294 HIV-specific antibodies were isolated using HIV antigen-coated plates (Murex HIV1.2.0 kit  
295 9E25-01, Diasorin, Schiphol-Rijk, The Netherlands). Sera were diluted two times in sample  
296 diluent from kit (50  $\mu$ L serum with 50  $\mu$ L diluent) and incubated for 1 hour at room  
297 temperature shaking 450 r.p.m. (Heidolph Titramax 100, Schwabach, Germany). As positive  
298 control, anti-HIV gp120 monoclonal was used (IgG1 b12; 100  $\mu$ g purified antibody in PBS at 1  
299 mg/ml; NIH Aids Reagent Program, La Jolla, CA, US). Washing and eluting specific antibodies

300 was done as described above for CMV-specific antibodies.

301

### 302 **Purification of ParvoB19-specific antibodies from sera**

303 ParvoB19-specific antibodies were isolated using ParvoB19 antigen-coated plates  
304 (Abcam1788650- Anti-Parvovirus B19 IgG ELISA, Cambridge, United Kingdom). Sera were  
305 diluted five times in sample diluent from kit (20  $\mu$ L serum with 80  $\mu$ L diluent) and incubated  
306 for 1 hour at room temperature shaking 450 r.p.m. (Heidolph Titramax 100). Positive and  
307 negative controls from the kit were used as controls. Washing and eluting specific antibodies  
308 was done as described above for CMV-specific antibodies.

309

### 310 **Purification of anti-N and anti-S specific antibodies from plasma**

311 SARS-Cov-2-specific antibodies were purified using antigen-coated plates (NUCN, Roskilde,  
312 Denmark). Plates were coated (over-night, 4°C) with recombinant trimerized spike protein  
313 produced as described recently (28) or N protein (accession number MN908947, produced in  
314 HEK cells with HAVT20 leader peptide, 10xhis tag and a Brit tag as in (23)) in PBS(5  $\mu$ g/mL  
315 and 1  $\mu$ g/mL, respectively). Plates were washed 3 $\times$  with PBS supplemented with 0.05 %  
316 TWEEN 20<sup>®</sup> (PBS-T) and plasma (20  $\mu$ L) diluted in PBS-T (180  $\mu$ L) was incubated on the  
317 plates(1 hour, 37 °C, shaking). Sera dating pre COVID-19 pandemic were used as negative  
318 controls. The plates were washed seven times: 3 $\times$  with PBS-T, 2 $\times$  with PBS and 2 $\times$  with  
319 ammonium bicarbonate (50mM). The bound antibodies were then eluted with formic acid  
320 (100 mM, 5 min, shaking).

321

### 322 **Purification of total IgG from sera**

323 Total IgG1 antibodies were captured from 2  $\mu$ L of serum using Protein G Sepharose 4 Fast  
324 Flow beads (GE Healthcare, Uppsala, Sweden) in a 96-well filter plate (Millipore Multiscreen,  
325 Amsterdam, The Netherlands) as described previously (11) or by using Protein G cartridges

326 on the AssayMAP Bravo (Agilent Technologies, Santa Clara, USA) Briefly, 1  $\mu$ L serum diluted in  
327 PBS were applied to the cartridges, followed by washes of PBS, LC-MS pure water and finally  
328 eluted with formic acid (1%).

329

### 330 **Mass spectrometric IgG-Fc glycosylation analysis**

331 Eluates containing either antigen-specific antibodies or total IgG were collected in V-bottom  
332 plates, dried by vacuum centrifugation for 2.5 hours at 50°C. The HPA1a, CMV, HIV, ParvoB19,  
333 HBV, and COVID-19 samples were then subjected to proteolytic cleavage using trypsin as  
334 described before (11). The measles and mumps cohort samples were dissolved in a buffer  
335 containing 0.4% sodium deoxycholate(SDC), 10mM TCEP, 40mM chloroacetamide, 100 mM  
336 TRIS pH8.5. After 10min incubation at 95C, 250 ng Trypsin in 50 mM ammonium bicarbonate  
337 was added. The digestion was stopped after an overnight incubation by acidifying to 2%  
338 formic acid. Prior to MS injection, SDC precipitates were removed by centrifuging samples at  
339 20 000 rcf for 30 minutes.

340 Analysis of IgG Fc-glycosylation was performed with nanoLC reverse phase (RP)-electrospray  
341 (ESI)- MS on an Ultimate 3000 RSLCnano system (Dionex/Thermo Scientific, Breda, The  
342 Netherlands) coupled to an amaZon speed ion trap MS (Bruker Daltonics, Bremen, Germany)  
343 (11) for all samples except for the Measles and mumps cohorts that were measured on a  
344 Impact HD quadrupole-time-of-flight MS (Bruker Daltonics). (Glyco-)peptides were trapped  
345 with 100% buffer A (0.1% formic acid in water) and separated on a 15 min 0-25% buffer B  
346 (95% acetonitrile, 5% water) linear gradient. In the current study we focused on IgG1,  
347 without analyzing IgG3 due to its possible interference with IgG2 and IgG4 at the  
348 glycopeptide level (29). Mass spectrometry results were extracted and evaluated using  
349 FlexAnalysis software (Bruker Daltonics) for all samples except for the Measles virus, and  
350 Mumps virus cohorts that were analyzed with Skyline software. Data was judged reliable  
351 when the sum of the signal intensities of all glycopeptide species (Table S1) was at least  
352 higher than background plus 10 times its standard deviation, otherwise the data was excluded



353 (11). The total level of glycan traits was calculated as described in Table S2.

354

### 355 **Statistical analysis**

356 Statistical analyses were performed using GraphPad Prism version 7.02 for Windows  
357 (GraphPad Software Inc., La Jolla, CA, [www.graphpad.com](http://www.graphpad.com)). To analyze whether Fc-  
358 fucosylation for total and antigen specific IgG differs between the tested cohorts, statistical  
359 analysis was performed using t tests. To investigate whether Fc-fucosylation profiles of two  
360 specific antibodies in the same individual are correlated statistical analysis was performed  
361 using a Pearson correlation. The level of significance was set at  $P < 0.05$ .

362

363 **Acknowledgments:** We thank prof. dr. R.J.M. ten Berge for helpful discussions. The  
364 Amsterdam Cohort Studies on HIV infection and AIDS, is a collaboration between the  
365 Amsterdam Health Service, the Academic Medical Centre of the University of Amsterdam  
366 and Sanquin Blood Supply Foundation. The ACS is part of the Netherlands HIV Monitoring  
367 Foundation and financially supported by the Netherlands National Institute for Public Health  
368 and the Environment. We are greatly indebted to all cohort participants for their continuous  
369 participation. **Funding:** This work was supported by LSBR grants number 1229 and 1908 (to  
370 G.V.) and by the European Union (Seventh Framework Programme HighGlycan project, grant  
371 number 278535 and H2020 projects GlySign, grant number 722095), and by the Netherlands  
372 Organization for Scientific Research (NWO) Vici grant (to R.W.S.)

373 **Author contributions:** All samples were collected by SN, SS, ST, AV, AB, RV, MB, TS, SB, FL, NK,  
374 HZ, and MS. MS, CK, RP, JN, ML and EdG performed antibody purifications, mass  
375 spectrometric analyses and data processing. FL, MB, TS, and PB, generated recombinant  
376 antigens, MS, EdG, GV, and EvdS analyzed clinical data and performed data analysis. ML, MS,  
377 EdG, MW and GV made figures and tables. MG, RS, EvdS, MW and GV supervised the study.  
378 All authors contributed to analysis and interpretation of the data. ML, MS, EdG, ES, MW and  
379 GV wrote the paper, which was critically revised and approved by all authors. **Competing**  
380 **interests:** The authors declare no competing interest. **Data and materials availability:** The  
381 data presented in this manuscript are in the main paper.

382

383

384 **References and Notes:**

- 385 1. M. H. C. Biermann *et al.*, Sweet but dangerous - the role of immunoglobulin G  
386 glycosylation in autoimmunity and inflammation. *Lupus*. **25**, 934–42 (2016).
- 387 2. R. Jefferis, Glycosylation as a strategy to improve antibody-based therapeutics. *Nat.*  
388 *Rev. Drug Discov.* **8**, 226–34 (2009).
- 389 3. G. Vidarsson, G. Dekkers, T. Rispens, IgG subclasses and allotypes: From structure to  
390 effector functions. *Front. Immunol.* **5**, 520 (2014).
- 391 4. G. Dekkers, T. Rispens, G. Vidarsson, Novel concepts of altered immunoglobulin G  
392 galactosylation in autoimmune diseases. *Front. Immunol.* **9**, 553 (2018).
- 393 5. R. L. Shields *et al.*, Lack of fucose on human IgG1 N-linked oligosaccharide improves  
394 binding to human FcγR3 and antibody-dependent cellular toxicity. *J Biol Chem.*  
395 **277**, 26733–26740 (2002).
- 396 6. C. Ferrara *et al.*, Unique carbohydrate-carbohydrate interactions are required for high  
397 affinity binding between FcγR3 and antibodies lacking core fucose. *Proc Natl*  
398 *Acad Sci U S A.* **108**, 12669–12674 (2011).
- 399 7. J. M. Reichert, Antibodies to watch in 2016. *MAbs.* **8**, 197–204 (2016).
- 400 8. M. P. Baković *et al.*, High-throughput IgG Fc N-glycosylation profiling by mass  
401 spectrometry of glycopeptides. *J. Proteome Res.* **12**, 821–31 (2013).
- 402 9. N. de Haan, K. R. Reiding, G. Driessen, M. van der Burg, M. Wuhrer, Changes in Healthy  
403 Human IgG Fc-Glycosylation after Birth and during Early Childhood. *J. Proteome Res.*  
404 **15**, 1853–61 (2016).
- 405 10. M. Wuhrer *et al.*, Regulated glycosylation patterns of IgG during alloimmune  
406 responses against human platelet antigens. *J Proteome Res.* **8**, 450–456 (2009).
- 407 11. R. Kapur *et al.*, A prominent lack of IgG1-Fc fucosylation of platelet alloantibodies in  
408 pregnancy. *Blood.* **123**, 471–480 (2014).
- 409 12. R. Kapur *et al.*, Low anti-RhD IgG-Fc-fucosylation in pregnancy: A new variable  
410 predicting severity in haemolytic disease of the fetus and newborn. *Br. J. Haematol.*  
411 **166**, 936–945 (2014).
- 412 13. M. E. Sonneveld *et al.*, Glycosylation pattern of anti-platelet IgG is stable during  
413 pregnancy and predicts clinical outcome in alloimmune thrombocytopenia. *Br. J.*  
414 *Haematol.* **174**, 310–320 (2016).
- 415 14. T. T. Wang *et al.*, IgG antibodies to dengue enhanced for FcγR3A binding determine  
416 disease severity. *Science.* **355**, 395–398 (2017).
- 417 15. M. E. Ackerman *et al.*, Natural variation in Fc glycosylation of HIV-specific antibodies  
418 impacts antiviral activity. *J Clin Invest.* **123**, 2183–2192 (2013).
- 419 16. M. H. J. Selman *et al.*, Changes in antigen-specific IgG1 Fc N-glycosylation upon  
420 influenza and tetanus vaccination. *Mol. Cell. Proteomics.* **11** (2012),  
421 doi:10.1074/mcp.M111.014563.

- 422 17. A. C. Vestrheim *et al.*, A pilot study showing differences in glycosylation patterns of IgG  
423 subclasses induced by pneumococcal, meningococcal, and two types of influenza  
424 vaccines. *Immun Inflamm Dis.* **2**, 76–91 (2014).
- 425 18. M. E. Sonneveld *et al.*, Antigen specificity determines anti-red blood cell IgG-Fc  
426 alloantibody glycosylation and thereby severity of haemolytic disease of the fetus and  
427 newborn. *Br. J. Haematol.* **176**, 651–660 (2017).
- 428 19. J. Krištić *et al.*, Glycans are a novel biomarker of chronological and biological ages. *J*  
429 *Gerontol A Biol Sci Med Sci.* **69**, 779–789 (2014).
- 430 20. L. Bouadma, F. X. Lescure, J. C. Lucet, Y. Yazdanpanah, J. F. Timsit, Severe SARS-CoV-2  
431 infections: practical considerations and management strategy for intensivists. *Intensive*  
432 *Care Med.* **46**, 579–582 (2020).
- 433 21. C. Huang *et al.*, Clinical features of patients infected with 2019 novel coronavirus in  
434 Wuhan, China. *Lancet.* **395**, 497–506 (2020).
- 435 22. T. T. Wang *et al.*, Anti-HA Glycoforms Drive B Cell Affinity Selection and Determine  
436 Influenza Vaccine Efficacy. *Cell.* **162**, 160–169 (2015).
- 437 23. G. Dekkers *et al.*, Decoding the human immunoglobulin G-glycan repertoire reveals a  
438 spectrum of Fc-receptor- and complement-mediated-effector activities. *Front.*  
439 *Immunol.* **8** (2017), doi:10.3389/fimmu.2017.00877.
- 440 24. A. Volz, G. Sutter, Modified Vaccinia Virus Ankara: History, Value in Basic Research, and  
441 Current Perspectives for Vaccine Development. *Adv. Virus Res.* **97**, 187–243 (2017).
- 442 25. L. Liu *et al.*, Anti-spike IgG causes severe acute lung injury by skewing macrophage  
443 responses during acute SARS-CoV infection. *JCI insight.* **4** (2019),  
444 doi:10.1172/jci.insight.123158.
- 445 26. B. D. Quinlan *et al.*, *bioRxiv*, in press, doi:10.1101/2020.04.10.036418.
- 446 27. Q. Ye, B. Wang, J. Mao, The pathogenesis and treatment of the ‘Cytokine Storm’ in  
447 COVID-19.’ *J. Infect.* (2020), , doi:10.1016/j.jinf.2020.03.037.
- 448 28. P. Brouwer *et al.*, *bioRxiv*, in press, doi:10.1101/2020.05.12.088716.
- 449 29. H. K. Einarsdottir *et al.*, Comparison of the Fc glycosylation of fetal and maternal  
450 immunoglobulin G. *Glycoconj. J.* **30**, 147–157 (2013).

451

452

# **Afucosylated immunoglobulin G responses are a hallmark of enveloped virus infections and show an exacerbated phenotype in COVID-19**

## **- Supplementary data -**

**Authors:** Mads Delbo Larsen<sup>1</sup>, Erik L. de Graaf<sup>1</sup>, Myrthe E. Sonneveld<sup>1</sup>, H. Rosina Plomp<sup>2</sup>, Federica Linty<sup>1</sup>, Remco Visser<sup>1</sup>, Max Brinkhaus<sup>1</sup>, Tonci Sustic<sup>1</sup>, Steven de Taeye<sup>1</sup>, Arthur Bentlage<sup>1</sup>, Jan Nouta<sup>2</sup>, Suvi Natunen<sup>3</sup>, Carolien A. M. Koeleman<sup>2</sup>, Susanna Sainio<sup>3</sup>, Neeltje A. Kootstra<sup>4</sup>, Philip Brouwer<sup>5</sup>, Rogier Sanders<sup>5</sup>, Marit van Gils<sup>5</sup>, Sanne de Bruin<sup>6</sup>, Alexander P.J. Vlaar<sup>6</sup>, Hans L. Zaaijer<sup>7</sup>, Manfred Wuhrer<sup>2</sup>, C. Ellen van der Schoot<sup>1</sup>, Gestur Vidarsson<sup>1</sup>

### **Affiliations:**

<sup>1</sup> Department of Experimental Immunohematology, Sanquin Research, Amsterdam, The Netherlands, and Landsteiner Laboratory, Amsterdam UMC, University of Amsterdam, Amsterdam, The Netherlands;

<sup>2</sup> Center for Proteomics and Metabolomics, Leiden University Medical Center, Leiden, The Netherlands;

<sup>3</sup> Finnish Red Cross Blood Service, Helsinki, Finland;

<sup>4</sup> Department of Experimental Immunology, Amsterdam UMC, University of Amsterdam Amsterdam, The Netherlands;

<sup>5</sup> Department of Medical Microbiology, Amsterdam University Medical Centers (Location AMC), University of Amsterdam, Amsterdam, The Netherlands;

<sup>6</sup> Department of Intensive Care Medicine, Amsterdam UMC (Location AMC), University of Amsterdam, Amsterdam, The Netherlands;

<sup>7</sup> Department of Blood-borne Infections, Sanquin, Amsterdam, The Netherlands.

# Larsen et al. Fig. S1.

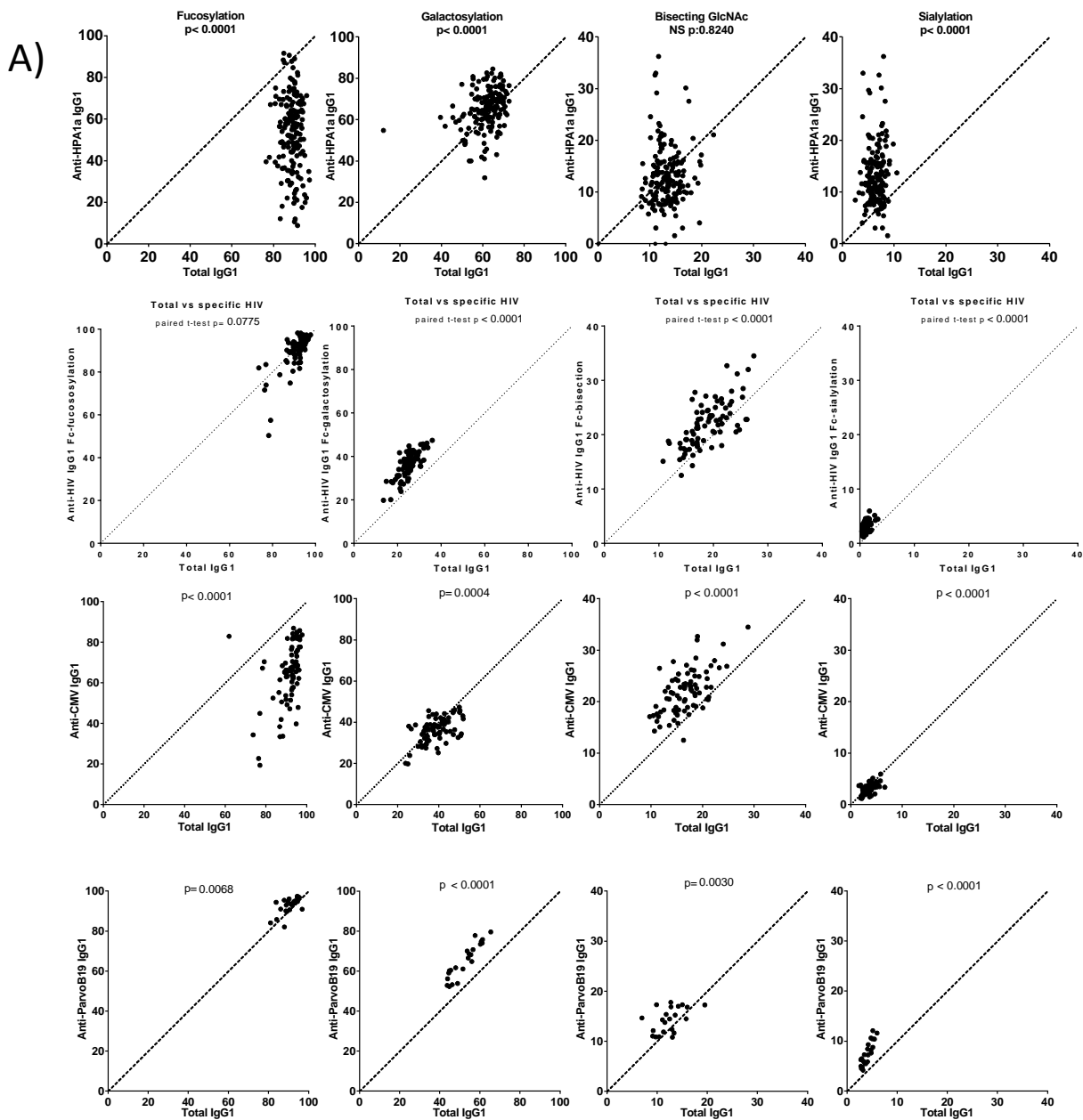


**Fig. S1: IgG1-glycosylation for A) anti-HPA-1a, HIV, CMV and Parvo-B19 and B) anti-Measles and Mumps (next page).**

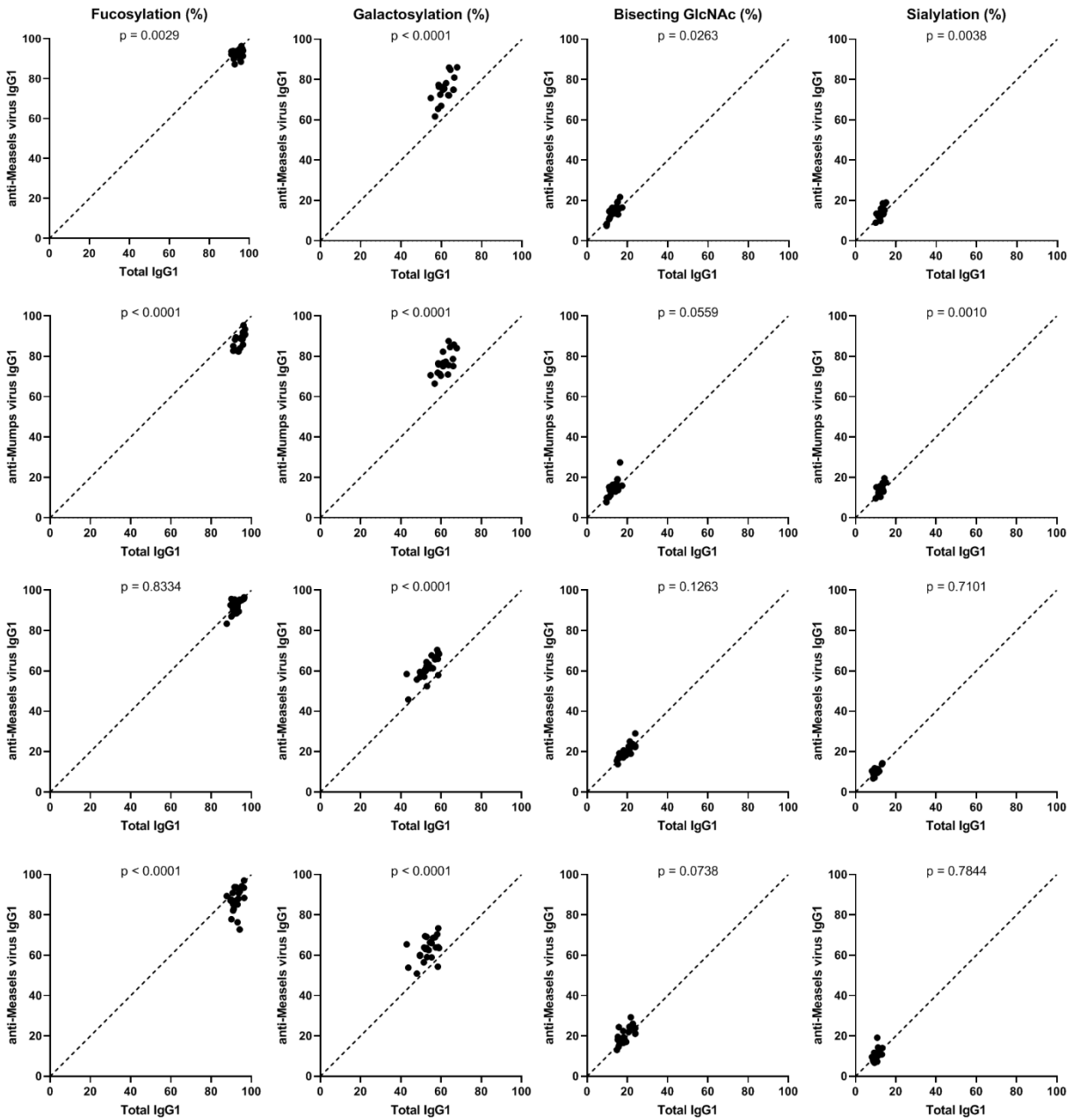
Shown are total IgG glycan traits (x-axis) vs the corresponding antigen-specific glycosylation on the Y-Axis for Fucosylation, Galactosylation, Bisection and sialylation.

Fig. S1 continued

B)

Vaccinees

Naturally infected



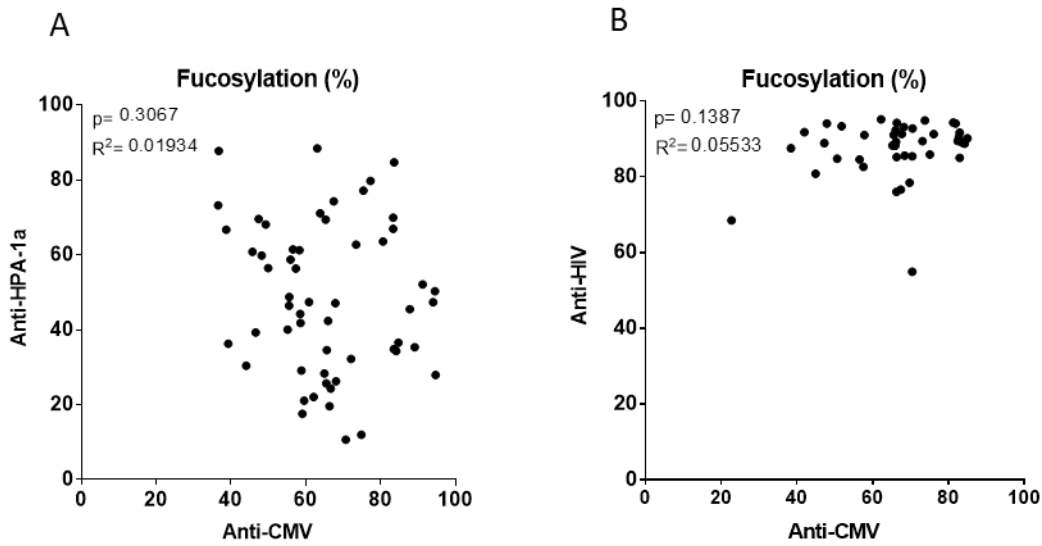


**Fig. S2. Antibody fucosylation is not determined by a general host factor. a.**

No correlation was found between the level of IgG1 Fc-fucosylation made during alloimmunization against HPA1a in pregnancy (y-axis) and CMV (x-axis) in the same individual. **b.** Also no correlation was found between the level of IgG1 Fc-fucosylation made against HIV (y-axis) and CMV (x-axis) in the same individual. Statistical analysis was performed using Pearson correlation.



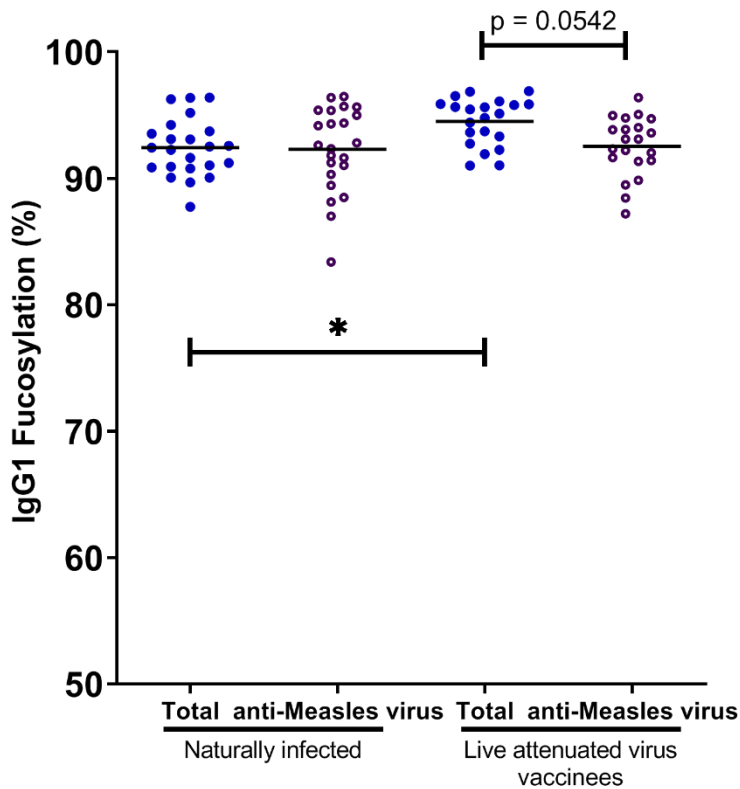


**Fig. S3: Fucosylation of anti-Measles.** Compared to total IgG fucosylation, the antigen-specific IgG fucosylation, of anti-measle antibodies was only significantly lowered in the younger vaccinated cohort (mean age 19.5). This is likely to be masked by the natural tendency of lowered total IgG-fucosylation with increasing age (9), as the naturally infected cohort (before introduction of the MeV/MuV vaccination program in 1980s in the Netherlands) is older than the vaccine cohort (average 63.5 vs 19.5 years, respectively). In line with this, the total IgG fucosylation of the older cohort showed significantly lowered total-IgG fucosylation compared to the younger vaccinated cohort / Statistical analysis was performed as paired t-test for A,B, and C and as a one-way ANOVA Sidak's multiple comparisons test comparing total IgG to antigen-specific IgG within groups, and same specificity IgG between groups, for D and E. Only statistically significant differences are shown. (\*=  $p < 0.1$  )

Supplementary Table 1. Overview of the IgG Fc glycopeptides which were included. The monoisotopic m/z value of the 2+ and 3+ charge state are shown, together with the average retention time determined for all N-glycans of each IgG subclass. Glycan compositions are denoted using the following nomenclature: H = hexose, N = N-acetylhexosamine; F = fucose; S = sialic (N-acetylneuraminic acids).

N-glycopeptides	m/z 2+	m/z 3+	retention time (s)
IgG1 H3N4F1S0 [G0F]	1317.526	878.687	336
IgG1 H4N4F1S0 [G1F]	1398.552	932.704	336
IgG1 H5N4F1S0 [G2F]	1479.579	986.722	336
IgG1 H3N5F1S0 [G0FN]	1419.066	946.380	336
IgG1 H4N5F1S0 [G1FN]	1500.092	1000.398	336
IgG1 H5N5F1S0 [G2FN]	1581.119	1054.415	336
IgG1 H3N4F0S0 [G0]	1244.497	830.001	336
IgG1 H4N4F0S0 [G1]	1325.524	884.018	336
IgG1 H5N4F0S0 [G2]	1406.550	938.036	336
IgG1 H3N5F0S0 [G0N]	1346.037	897.694	336
IgG1 H4N5F0S0 [G1N]	1427.063	951.712	336
IgG1 H5N5F0S0 [G2N]	1508.090	1005.729	336
IgG1 H4N4F1S1 [G1FS]	1544.100	1029.736	396
IgG1 H5N4F1S1 [G2FS]	1625.127	1083.754	396
IgG1 H4N5F1S1 [G1FNS]	1645.640	1097.429	396
IgG1 H5N5F1S1 [G2FNS]	1726.667	1151.447	396
IgG1 H4N4F0S1 [G1S]	1471.071	981.050	396
IgG1 H5N4F0S1 [G2S]	1552.098	1035.068	396
IgG1 H4N5F0S1 [G1NS]	1572.611	1048.743	396
IgG1 H5N5F0S1 [G2NS]	1653.638	1102.7610	396
IgG1 H5N4F1S2 [G2FS2]	1770.675	1180.786	396

# Supplementary Table 2.

Supplemental Table 2. An overview of the calculations for the derived glycosylation traits.		
Derived trait	Definition	Calculation
Fucosylation	% of N-glycans which carry a core fucose	$\frac{[H3N4F1S0 + H4N4F1S0 + H5N4F1S0 + H3N5F1S0 + H4N5F1S0 + H5N5F1S0 + H4N4F1S1 + H5N4F1S1 + H4N5F1S1 + H5N5F1S1 + H5N4F1S2]}{\text{Sum of all glyco species}}$
Galactosylation	% of N-glycans which carry a galactose	$\frac{[(H5N4F1S0 + H5N5F1S0 + H5N4F0S0 + H5N5F0S0 + H5N4F1S1 + H5N5F1S1 + H5N4F0S1 + H5N5F0S1 + H5N4F1S2) + 0.5 * (H4N4F1S0 + H4N5F1S0 + H4N4F0S0 + H4N5F0S0 + H4N4F1S1 + H4N5F1S1 + H4N4F0S1 + H4N5F0S1)]}{\text{Sum of all glyco species}}$
Sialylation	% of N-glycans which carry a N-acetylneuraminic (sialic) acid	$\frac{[H5N4F1S2 + 0.5 * (H4N4F1S1 + H5N4F1S1 + H4N5F1S1 + H5N5F1S1 + H4N4F0S1 + H5N4F0S1 + H4N5F0S1 + H5N5F0S1)]}{\text{Sum of all glyco species}}$
Bisection	% of N-glycans which carry a bisecting N-acetylglucosamine	$\frac{[H3N5F1S0 + H4N5F1S0 + H5N5F1S0 + H3N5F0S0 + H4N5F0S0 + H5N5F0S0 + H4N5F1S1 + H5N5F1S1 + H4N5F0S1 + H5N5F0S1]}{\text{Sum of all glyco species}}$